

# A Deep Learning-Based Method for Power System Resilience Evaluation

Xuesong Wang, *Student Member, IEEE*, and Caisheng Wang, *Fellow, IEEE*

**Abstract**—Power systems are critical infrastructure in modern society, and power outages can cause significant disruptions to communities and individuals’ daily lives. The resilience of a power system measures its ability to maintain power supply during highly disruptive events such as hurricanes, earthquakes, and thunderstorms. Traditional methods for quantifying power system resilience include statistics-based and simulation-based approaches. Statistics-based methods offer a retrospective analysis of system performance without requiring a physical model, while simulation-based methods necessitate detailed physical system information and often simplify real-world scenarios. This paper introduces a deep learning-based method for evaluating power system resilience using historical power outage data. The method leverages the generalization capabilities of deep learning models and incorporates socio-economic and demographic factors as weighting terms to highlight the impacts on vulnerable demographic groups. The effectiveness of the proposed method is demonstrated through two case studies: one with real historical outage data and the other with simulated outage records. This approach provides valuable insights into measuring power system resilience against hazardous weather events without requiring a physical model of the target systems. The evaluation results can further guide the planning of distributed energy resources for resilience enhancement.

**Index Terms**—deep learning, evaluation, power system, resilience.

## I. INTRODUCTION

**E**LECTRIC power is essential in any modern society, and power outages can cause significant economic and social losses, and even life threatening consequences. Notably, 80% of major U.S. power outages reported from 2000 to 2023 were due to weather-related events [1]. Additionally, the number of weather-related power outages is on the rise, with twice as many occurring during 2014-2023 compared to 2000-2009 [1]. Due to this trend, understanding the characteristics of power outages under different scenarios is critical. To study power system characteristics under disruptive events, two concepts, reliability and resilience, have been proposed [2]. Reliability emphasizes adequacy and security [2], [3], [4]. Adequacy refers to the uninterrupted power supply, ensuring continuous service to end-users, while security is the capability to withstand unexpected disruptions, such as sudden power loss

caused by component failure and adverse weather [5]. Reliability typically addresses high-probability, low-impact (HPLI) events, whereas resilience focuses on low-probability, high-impact (LPHI) events [2]. Resilience relates to the system’s capability to maintain power supply during highly disruptive events, such as hurricanes, earthquakes, flooding, and cyber-physical attacks [2], [6].

Researchers have developed statistics-based and simulation-based methods to assess power system resilience [7]. Statistics-based methods create statistical terms to describe system characteristics using historical power outage records [8]. These methods do not require physical models of the power system, such as system topology or fragility models, and provide a retrospective summary of system performance. However, due to the rarity of LPHI events, statistics-based methods are typically applied to case studies of specific events, such as hurricanes. Moreover, comparing resilience evaluations across different systems can be challenging if the studied regions have not experienced similar weather events. Simulation-based methods simulate the power system using physical models and study system performance under specific scenarios based on detailed information like system topology and component fragility models [9]. In simulation-based methods, resilience is often measured using the resilience trapezoid [10] over multiple rounds of Monte Carlo simulation. These methods generate hazard scenarios from known models and fixed distributions, providing a benchmark for fair comparisons across distinct systems. Although simulation-based methods do not require extensive historical power outage records, they often oversimplify real-world scenarios. Furthermore, accurate topology and fragility curve information is challenging to obtain for simulation-based methods.

The performance of a physical system tells only half of the story. Different demographic groups experience varying levels of vulnerability even when facing the same power outage. A three-dimensional metric of social vulnerability—health, preparedness, and evacuation intention and means—was proposed to quantify the degree to which a person’s life or livelihood is put at risk by a long-duration power outage [11], [12]. Similarly, a statistical analysis of power outages experienced after Hurricane Hermine in Tallahassee, FL, studied different socio-demographic segments of the population [13]. A hybrid approach was proposed to combine community and infrastructure capitals into an Area Resilience metric, called AREZ [14]. It captured the role and impact of both infrastructure and community by integrating five sectors: energy, public health, natural ecosystem, socio-economic, and transportation.

In this work, we propose a deep learning-based method

X. Wang and C. Wang are with the Department of Electrical and Computer Engineering, Wayne State University, Detroit, MI 48202 USA, e-mail: xswang@wayne.edu; cwang@wayne.edu. (Corresponding author: Caisheng Wang.)

This material is based upon work supported by the Department of Energy, Solar Energy Technologies Office (SETO) Renewables Advancing Community Energy Resilience (RACER) program under Award Number DE-EE0010413. Any opinions, findings, conclusions, or recommendations expressed in this material are those of the authors and do not necessarily reflect the views of the Department of Energy.

for power system resilience evaluation that combines the advantages of both statistics-based and simulation-based methods and also considers the social vulnerability of different demographic groups. We first trained a deep neural network to learn the system performance, as measured by the resilience trapezoid [9], given a weather scenario. Then, we built a benchmark weather scenario dataset. The power system resilience of all the studied regions was tested using the trained model against the benchmark weather scenario dataset. Finally, the evaluation results were weighted using the socio-economic and demographic factors of the studied regions.

The remainder of this paper is organized as follows. Section II reviews statistics-based and simulation-based methods and the application of deep learning to power system resilience evaluation. The proposed deep learning-based method is detailed in Section III. Two case studies are presented in Section IV to demonstrate the proposed method. Finally, Section V concludes the paper.

## II. RELATED WORK

### A. Statistics-based Methods for Resilience Evaluation

Statistics-based methods for resilience evaluation typically compose resilience metrics using various demographic, social, and economic indicators. For example, the authors of [15] proposed a framework to assess technical, social, and economic resilience in rural power systems based on 42 selected indicators, including 21 for technical resilience, 8 for social resilience, and 13 for economic resilience. However, [15] did not provide a case study.

The Environment for Analysis of Geo-Located Energy Information (EAGLE-I) dataset contains detailed records of power outages across U.S. counties from 2014 to 2022 [16]. Using this dataset, studies [17] and [18] introduced various metrics to assess the performance of the power grid during extreme outage events, including event duration, impact duration, recovery duration, post-event duration, impact level, impact rate, recovery rate, and the recovery-to-impact ratio. Each metric was represented by a corresponding probability distribution function. While [17] and [18] did not incorporate weather data, the study [19] combined the EAGLE-I dataset with publicly available data from the National Weather Service to evaluate power system resilience using three metrics: Time Over Threshold (TOT), Area Under the Curve (AUC), and Time After the End of the event (TAE). This analysis explored power system resilience at state and county levels across various weather event types.

The U.S. Department of Energy (DOE) collects information on the reliability of power systems through the Electric Emergency Incident and Disturbance Report (Form DOE 417). The authors of [20] conducted statistical trend tests for power system resilience, including analyzing the rate of disruptions, a proposed composite resilience measure, performance loss, and recovery time, using Form DOE 417 data from 2002 to 2016. A regression analysis was conducted on these metrics with 41 explanatory variables. The authors of [21] examined the key factors affecting power system resilience under severe weather-induced disruptions, considering three dimensions:

extrinsic disruptions, the intrinsic capacities of a system, and the effectiveness of recovery, using Form DOE 417 data from 2007 to 2018.

Statistics-based methods for power system resilience evaluation have their pros and cons. Since these methods use historical power outage data, the analysis results accurately reflect real-world scenarios. However, because different regions experience different weather events, it can be challenging to make fair comparisons of resilience between regions.

### B. Simulation-Based Methods for Resilience Evaluation

Simulation-based methods typically comprise three models: a system model, a hazard model, and a fragility model [22], [23], [24], [25], [26]. The behavior of the system components is determined by the component characteristics, the hazard profile, and the fragility model. For each hazard applied to the system, the system's performance is recorded to calculate the system resilience metrics [27].

The fragility model can be developed from recorded historical outage events or through physical modeling. The fragility model in [8] was developed based on Hurricane Hermine power outage data. Monte Carlo simulation was utilized to estimate the potential impacts of two resilience policy/investment decisions: investing in infrastructure component upgrade and replacement and reducing component restoration time for faster recovery. The fragility of distribution components subjected to ice storms was investigated through physical modeling, considering four different failure modes and the effect of wind attack angle in [24].

In some works, reliability and resilience have been jointly studied [28], [29]. Resilience can also be analyzed for interconnected infrastructure systems. For example, resilience has been examined in energy systems, including gas, heat, and power [30], [31], [32], [33]. Similarly, resilience has been studied in power, gas, and water systems in [34]. The authors of [35] proposed InfraRisk, a simulation platform designed to study interconnected power-water-transport systems.

There are advantages and disadvantages to simulation-based methods for power system resilience evaluation. One significant advantage is that we can fully model system behavior using a system model, an attack model, and a fragility model. This capability allows for multiple simulations with varying parameters, providing an excellent opportunity to compare the resilience of different system designs and enhancement strategies. However, a notable disadvantage is that the developed model often oversimplifies real-world scenarios. As a result, simulation-based methods may only provide theoretical results, which can significantly differ from actual real-world situations.

### C. Deep Learning Application to Power System Resilience Evaluation

Some researchers applied deep learning techniques to power outage prediction. In [36], the application of machine learning in power system resilience was reviewed. Machine learning-based outage prediction models were proposed in [37] to identify relevant weather events and quantify the associated outages using data from the European Centre for Medium-Range

Weather Forecasts Reanalysis v5 (ERA5 and ERA5-Land). In [38], a tree-based ensemble machine learning method was proposed for outage prediction. Targeting multivariate disaster data, [39] used a feed-forward neural network and a Gated Recurrent Unit (GRU) to extract features of static and dynamic variables, respectively, and then employed a multi-head attention network to fuse all features, establishing a mapping relationship with the total number of line interruptions. In [40], machine learning models were proposed to predict outages using EAGLE-I data.

Deep learning techniques can also be utilized in simulation-based methods for studying power system resilience. The authors of [9] proposed using a Recurrent Neural Network to generate typhoon scenarios and applied them to an IEEE 13-bus system projected to a southeastern coastal area of China. The resilience was measured by the load shedding that occurred after some components were disrupted under a typhoon scenario. In [41], a Graph Neural Network was used to identify critical nodes and links, aiding in the study of power system resilience.

In this study, deep learning models are utilized to predict system performance, as measured by the resilience trapezoid, given the system information and weather scenario data. The weather inputs for the model in the proposed method specifically pertain to severe weather events. In contrast, models designed for power outage prediction applications handle both typical and severe weather events.

### III. METHODOLOGY

#### A. Method Overview

Our proposed method for evaluating power system resilience combines the advantages of both statistics-based and simulation-based methods. It treats the power system as a black box, and no detailed system topology is required. The system characteristics under severe weather scenarios are learned by a deep learning model using historical power outage records and weather data; hence, no fragility model is needed. After training the model, we input hazardous weather events and system information to predict system performance. The resilience of the system is then calculated as the average system performance across these test scenarios. Since multiple systems can be tested with the same set of attack events, this approach facilitates the comparison of resilience between different systems.

In this method, system performance is represented as the number of customers served, normalized by the total number of customers in the system; thus, the system performance is maximized at 1.0. When a severe weather event impacts the power system, performance initially drops, then plateaus while waiting for damaged components to be repaired, and finally restores to the initial system capacity after repairs, as illustrated in Fig. 1. The resilience of the system during a single event can be measured using the resilience trapezoid method [10], as shown in (1). Here,  $Rs_{i,k}$  represents the resilience of system  $k$  during outage event  $i$ ,  $f(t)$  denotes the normalized system performance curve during the event, and  $T_1$  and  $T_2$  are the start and end times of the outage

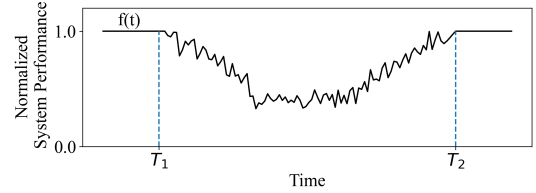


Fig. 1. Demonstration of the system performance curve under a hazardous weather event.  $f(t)$  is the normalized system performance curve.  $T_1$  and  $T_2$  are the start and end times of the outage event, respectively.

event, respectively. It is important to note that the end time of the outage event differs from the end time of the weather event; the former refers to when the system is fully recovered, while the latter marks the end of the weather scenario (e.g., a thunderstorm). Typically, the system recovery time extends beyond the weather event as it takes time for repair crews to fix all the damaged components. Depending on data availability, the end time of the weather event could also be used. In this method, a deep learning model is trained to predict  $Rs_{i,k}$  based on the system and weather event information, as detailed in Section III-B.

$$Rs_{i,k} = \frac{\int_{T_1}^{T_2} f(t) dt}{\int_{T_1}^{T_2} \mathbf{1} dt} = \frac{\int_{T_1}^{T_2} f(t) dt}{T_2 - T_1} \quad (1)$$

To comprehensively measure the resilience of a power system, a benchmark weather dataset is created that contains a set of hazardous weather events. The systems under study are tested using this benchmark dataset, and system resilience is calculated using (2), where  $Ru_k$  represents the unweighted resilience of power system  $k$ , and  $N_a$  is the number of hazardous weather events in the benchmark dataset. The range of unweighted resilience is between 0 and 1. The higher the  $Ru_k$ , the more resilient power system  $k$  is.

$$Ru_k = \frac{1}{N_a} \sum_{i=1}^{N_a} Rs_{i,k} \quad (2)$$

The unweighted resilience only considers the physical system's power outage, while different demographic groups may perceive power outages at varying levels. For example, a person with a disability might be more impacted compared to those without. To address this, a weighted resilience metric for the power system is proposed, where the unweighted resilience is adjusted with an exponential term based on social vulnerability factors in three dimensions, as proposed in [11]. This adjustment is detailed in (3), where  $Rw_k$  represents the weighted resilience of power system  $k$ ,  $N_w$  is the number of socio-economic and demographic factors ( $N_w = 15$  in this work), and  $W_{j,k}$  is factor  $j$  for power system  $k$ ,  $\lambda$  is a weighting coefficient that controls the impact of the factors on the weighted resilience ( $\lambda = \frac{1}{3}$  in this work). This work utilizes 15 socio-economic and demographic factors, as shown in Table I. The factors are normalized accordingly; for example, if the factors relate to the number of households, they are normalized by the total number of households in the

target region; if they pertain to the number of individuals, they are normalized by the population size in the region.

It is important to note that because the unweighted resilience ranges between 0 and 1 and all factors are positive, larger socio-economic and demographic factors result in smaller values of weighted resilience, indicating a less resilient system. This approach underscores the principle that regions with more socially vulnerable people are less resilient. Additionally, the weighting factors reflect human consideration of different population groups. If necessary, the weighting method can be adapted to emphasize the welfare of specific population groups, as demonstrated in case study A.

$$Rw_k = Ru_k^{[1+\lambda \sum_{j=1}^{N_w} W_{j,k}]} \quad (3)$$

## B. Model Design

A deep learning model is designed to estimate  $Rs_{i,k}$  given the weather event  $i$  and the characteristics of power system  $k$ . The model comprises an encoder and a decoder, as illustrated in Fig. 2. The encoder learns a universal weather embedding, while the decoder predicts the impact of the weather on the target system.

The input to the encoder is a concatenation of the weather sequence and the time embedding. The inclusion of a time embedding is useful when the benchmark dataset contains weather events from different times of the year. The encoder outputs an embedding representing the given weather scenario. Due to the variable lengths of the weather events, a Recurrent Neural Network is utilized.

The decoder receives the weather scenario embedding  $i$  extracted by the encoder and the power system embedding  $k$ . The output of the decoder is  $\hat{R}s_{i,k}$ , the predicted value of  $Rs_{i,k}$ . For simplicity, the architecture of the decoder is a multi-layer perceptron (MLP).

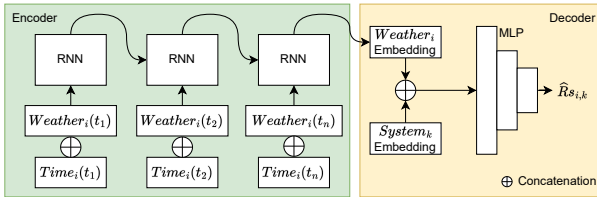


Fig. 2. Model architecture for predicting  $Rs_{i,k}$ , i.e., the resilience of the power system  $k$  under weather event  $i$ , where  $\hat{R}s_{i,k}$  is the predicted value of  $Rs_{i,k}$ .

## IV. CASE STUDIES

In this section, we apply the proposed method to evaluate the resilience of power systems in two case studies. In the first case study, the method was applied to a real-world power outage dataset at the county level in Michigan. In the second case study, we developed a simulation framework to produce system performance records at the substation service area level, and then the generated data was utilized in the proposed method.

### A. Case Study A

1) *Data Collection and Preprocessing*: To train the proposed deep learning model, we utilized the power outage data collected in the EAGLE-I dataset [16] to generate the ground truth  $Rs_{i,k}$ . First, we extracted all power outages for Michigan counties and downsampled the data from 15-minute intervals to hourly resolution. Three counties were removed because their first outages appeared in December 2019, which might indicate that these counties were added to the EAGLE-I system much later than the others. The authors of [18] noted that the outage numbers recorded by EAGLE-I do not represent the actual individuals served and converted the outage numbers into individuals using a scale of 2. We adopted the same approach in this work. We normalized the scaled numbers by the population size of the county in the corresponding year.

The goal of this work is not outage prediction for any weather scenarios but rather the estimation of power system resilience under LPHI events. Therefore, we filtered out all the normalized outages smaller than 0.1, selecting only the hours when at least 10% of the population lost power. If the time gap between any consecutive power outage periods in the same county was no more than 3 hours, we merged the two periods into one, and the missing data was linearly interpolated as needed. All outage events lasting less than 6 hours were removed. Any counties with fewer than 2 events were excluded to ensure that every county appeared in both the training and validation sets. This process resulted in a dataset that includes 71 counties in Michigan and a total of 682 events from 2014 to 2022. We calculated  $Rs_{i,k}$  for the 682 events as the ground truth for training.

The weather data was extracted from the High-Resolution Rapid Refresh (HRRR) model's output [43], [44], [45], facilitated by Herbie [46]. The HRRR model is an advanced numerical weather prediction system developed by the National Oceanic and Atmospheric Administration (NOAA). It is designed to provide high-resolution, frequently updated weather forecasts, focusing on the continental United States, Canada, and Mexico. We utilized 18 surface variables sampled at the population center of each county for each hour of the weather events. The 18 variables include wind gust, precipitation rate, snow depth, snow cover, pressure, temperature, total precipitation, visibility, and others. Missing values were filled with the value at the nearest timestamp. All the variables were normalized to a range between 0 and 1.

Most socio-economic and demographic factors used for weighted resilience were sourced from the American Community Survey 5-Year Estimates for 2022, except for the data on nursing home residents, which was taken from the 2020 Decennial Census, and the data on residents who rely on electricity-dependent medical equipment, which was sourced from HHS emPOWER [42], as summarized in Table I. The numbers were normalized by the total number of households or populations in each county, depending on the type of factors.

2) *Model Training and Validation*: We conducted 5-fold cross-validation when training the model, and the models with the best validation performance were saved and utilized in the resilience evaluation step. For simplicity, the embedding for



TABLE I  
SOCIO-ECONOMIC AND DEMOGRAPHIC FACTORS FOR WEIGHTED POWER RESILIENCE

Dimension	Factor	Data Source Used in Case Study A
Evacuation	Households without access to vehicles	American Community Survey B08201
	People whose work requires them to stay in the area during an outage	American Community Survey DP03
	People with a disability	American Community Survey S1810
Preparedness	Younger adults	American Community Survey S0101
	People who speak limited English	American Community Survey S1602
	Households with children	American Community Survey S1101
	Less educated adults	American Community Survey S1501
	Low-income households	American Community Survey DP03
	Elderly adults who live alone	American Community Survey B25011
Health	People who live in multi-family housing units	American Community Survey S1101
	Older adults (above 65)	American Community Survey S1810
	Children (below 5)	American Community Survey S1810
	Residents who rely on electricity-dependent medical equipment	HHS emPOWER [42]
	Nursing home residents	Decennial Census P5
	People with mobility limitations	American Community Survey S1810

TABLE II  
SEARCH SPACE OF THE HYPERPARAMETERS AND THE BEST HYPERPARAMETERS SEARCHED FOR CASE STUDY A

Hyperparameter	Search Space	Search Result
GRU hidden layer size	[32, 64, 128, 256]	128
Number of GRU layers	[1, 2, 3, 4]	1
Number of MLP layers	[1, 2, 3, 4]	2
GRU dropout rate	0.0 - 0.8	0.0
MLP dropout rate	0.0 - 0.8	0.2
Learning rate	1e-4 - 1e-2	0.00623
Weight decay	1e-5 - 1e-2	0.00058

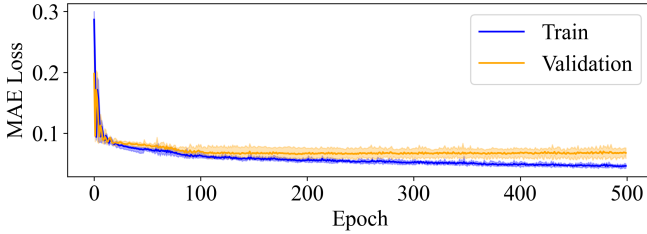


Fig. 3. Training and validation losses of case study A, averaged over the 5 folds.

the system is a one-hot encoding of the county. The Gated Recurrent Unit (GRU) [47] was chosen as the instance of the Recurrent Neural Network. All the models were trained for 500 epochs, with the Mean Absolute Error (MAE) loss function. The model was trained using the Adam optimizer [48].

To identify the best hyperparameters, we conducted a hyperparameter search using Ray Tune [49] and Optuna [50]. The search space for the hyperparameters and the best hyperparameters found are listed in Table II. All further analyses were carried out using the best hyperparameters identified in the search.

The training loss and validation loss, averaged over the 5 folds, are visualized in Fig. 3. The average validation loss of the best models over the 5 folds is 0.06301.

3) *Resilience Evaluation*: The benchmark dataset of weather scenarios was developed using all the weather events across all counties from 2020 to 2022, totaling 370 events. We

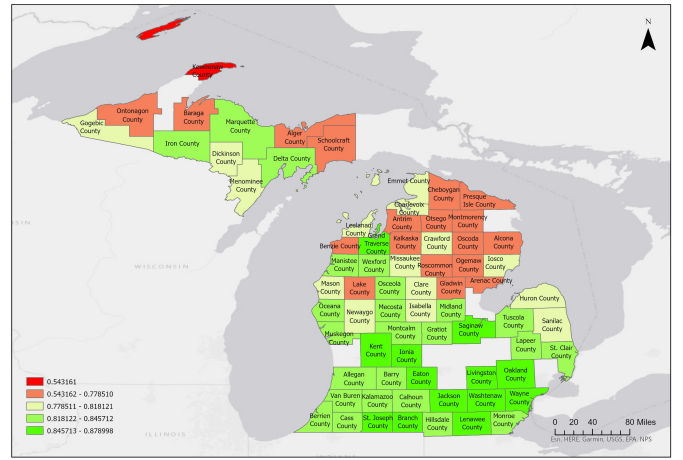


Fig. 4. Unweighted electric power resilience of 71 counties in Michigan.

tested all the counties against the benchmark dataset and used (2) and (3) to calculate the unweighted and weighted resilience for each county, as shown in Fig. 4 and Fig. 5, respectively. The rankings of the unweighted and weighted resilience for 71 counties in Michigan are shown in Fig. 6. The Spearman rank-order correlation coefficient between unweighted and weight resilience values is 0.99 ( $p = 8 * 10^{-62}$ ), which indicates that the weight terms did not change the overall rankings significantly.

As we discussed in Section III-A, the weight terms are subjective and reflect human consideration of different population groups. Besides summing up the factors, we can emphasize different population groups in the weight term. Here, we provide two examples to demonstrate the effect of such adjustments on the final weighted resilience rankings. In the first example, we assign greater weights (5) to three population groups: people with a disability, elderly individuals living alone, and low-income households. In the second example, inspired by [14], a penalty term of 3 was introduced to factors exceeding 0.2. The intuition is that counties with highly concentrated vulnerable groups should be considered less resilient. The results of the two examples are shown in Fig. 7. The Spearman rank-order correlation coefficients between the



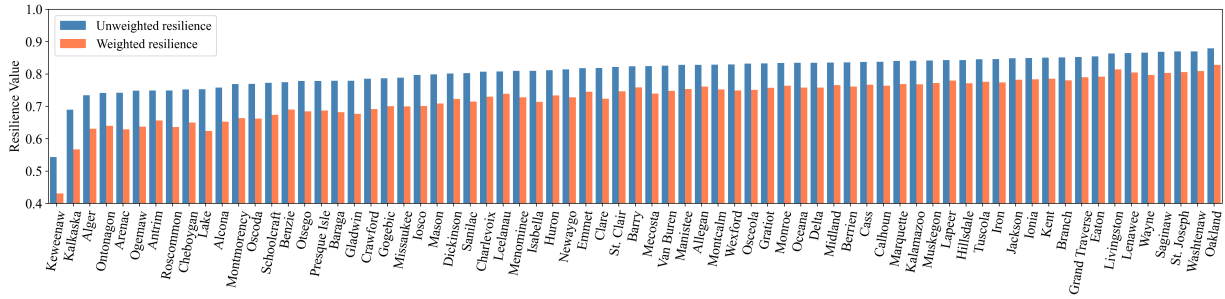


Fig. 6. Unweighted and weighted electric power resilience of 71 counties in Michigan.

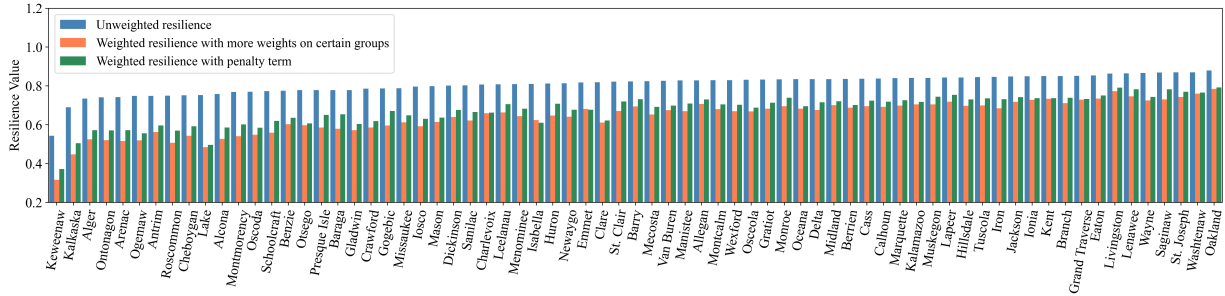


Fig. 7. Two examples of weighting methods. 1) weighted resilience with more weights on three population groups. 2) weighted resilience with more weights on factors larger than 0.2.

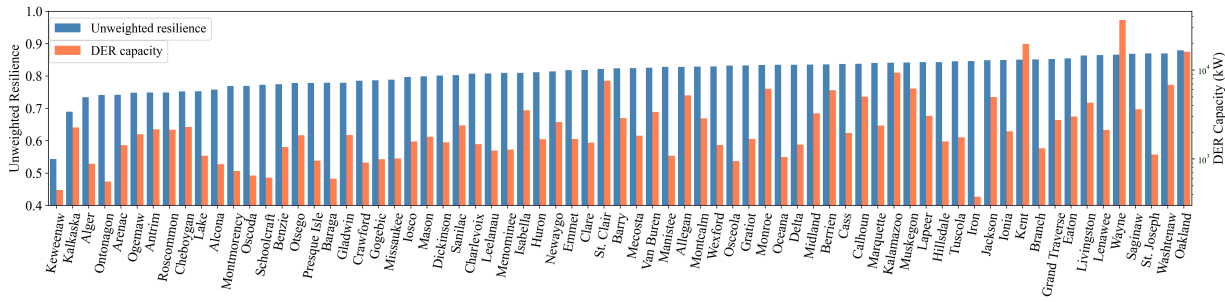


Fig. 8. Minimum capacity of DERs to be installed to enhance the unweighted resilience to 0.9 for each county.

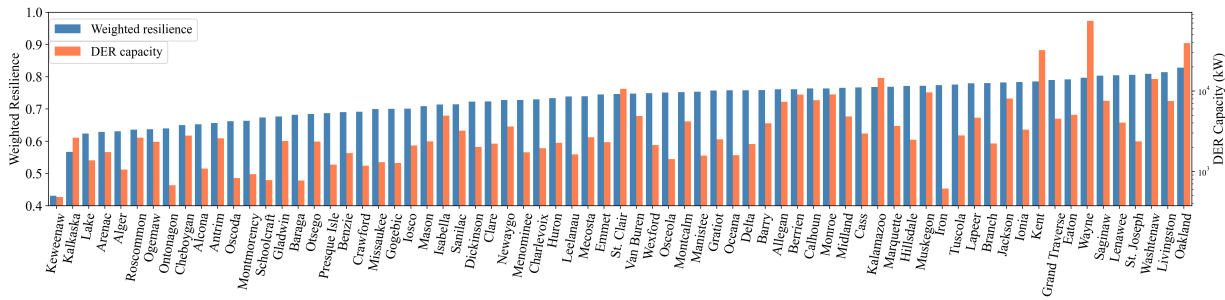


Fig. 9. Minimum capacity of DERs to be installed to enhance the weighted resilience to 0.9 for each county.

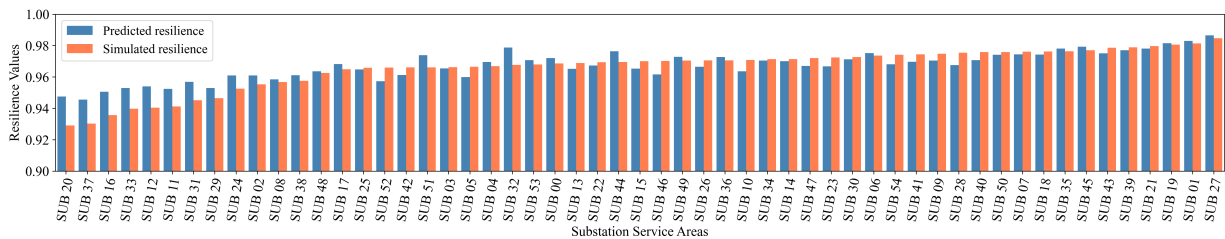


Fig. 10. Resilience values from simulation results and the model prediction.

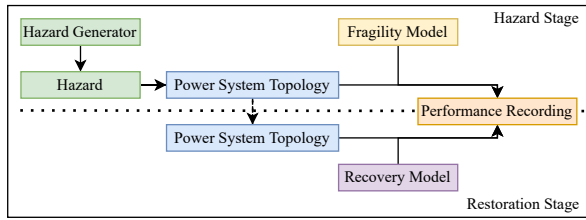


Fig. 11. Architecture of the simulation framework in case study B.

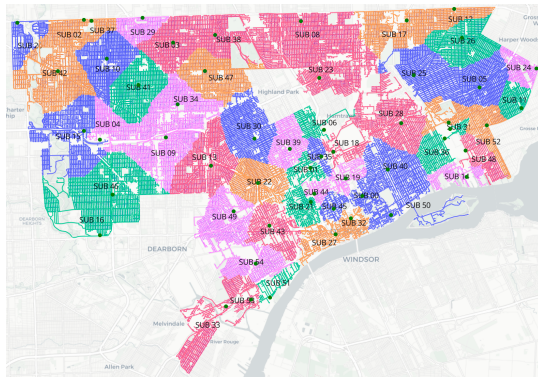


Fig. 12. Power system topology for Detroit generated using publicly available data, composed of poles, lines, substations, and buildings. Green dots are substations. Lines of different colors belong to different substation service areas.

3) *Hazard Generator*: The hazard considered in this case is wind during thunderstorms. We focused solely on wind speed and did not consider the impact of wind direction on the fragility of power lines. There are two distinct types of wind based on their duration and speed: wind gusts and sustained winds. Severe thunderstorms typically feature one or more high-speed wind gusts. For each generated hazard scenario, we predetermined the hours and substation service areas where the wind gusts would occur. In this case study, we assume that only power lines can be broken. The wind speed at the center of the lines is used to calculate the breaking probability. To generate the wind speed for each line, the hazard generator operates in two steps:

- A sparse wind speed field is generated.
- The wind speed for each line is calculated by interpolating the sparse wind speed field.

To generate the sparse wind speed field, a random location is drawn from each substation service area, and the wind speed at that location is randomly determined using the corresponding wind speed distribution, depending on whether it is a wind gust or a sustained wind point. The wind speed distribution of wind gusts is fitted using historical thunderstorm data from Wayne County, MI, spanning from 2010 to 2023. The wind speed distribution of sustained winds is fitted using the wind speed data from the same set of thunderstorms in Wayne County, as provided by the HRRR model. The speed distribution of wind gust and sustained wind are shown in Fig. 13. To expedite the interpolation process, we segmented the area into patches and assumed that the wind speed within each patch is constant.

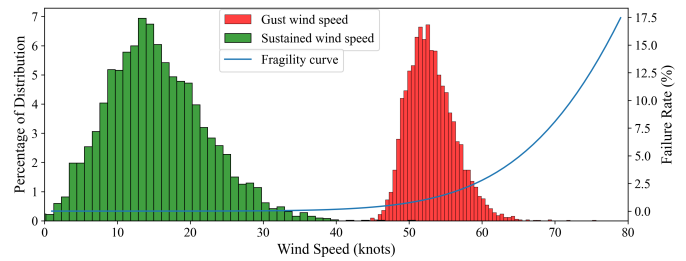


Fig. 13. Wind speed distribution and the fragility curve of distribution lines in terms of wind speed.

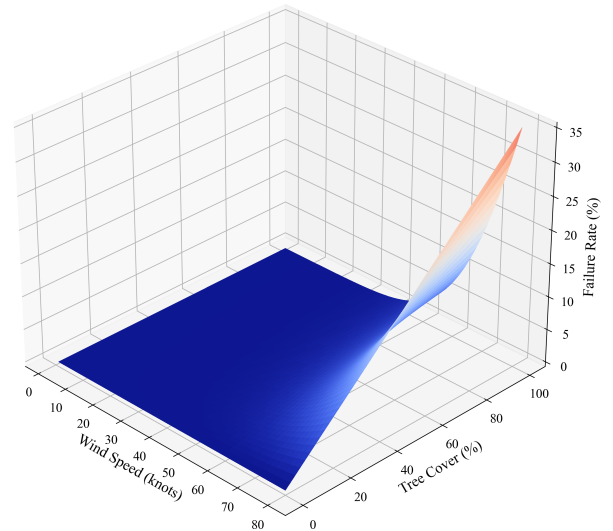


Fig. 14. Fragility model of distribution lines of joint impact of wind speed and tree coverage.

4) *Fragility Model*: This study considers two failure modes for power lines: damage due to wind speed alone and damage caused by fallen tree branches during thunderstorm winds. It is important to note that due to data limitations, we do not have the true distribution of failure rates; thus, the fragility curve shown in this example is for demonstration purposes only. The fragility curve of distribution lines under different wind speeds is shown in Fig. 13. To incorporate the second failure mode, tree coverage for each power line is sampled from a public dataset<sup>1</sup>. The fragility model for fallen tree branches in thunderstorm winds is shown in Fig. 14. The failure of all distribution lines is considered independent. When a line is broken, it is removed from the power system topology.

5) *Recovery Model*: We assume there are 15 repair teams shared by all the substation service areas. For each episode, the initial locations of the 15 repair teams are determined using K-Means clustering of the centroids of the substation service areas. During the hazard stage, the repair teams do not repair the damaged lines. In the restoration stage, the repair teams begin repairing the broken lines. The order in which lines are repaired is determined by their criticality, which is calculated

<sup>1</sup><https://data.fs.usda.gov/geodata/rastergateway/treecanopycover>

TABLE III  
SEARCH SPACE OF THE HYPERPARAMETERS AND THE BEST  
HYPERPARAMETERS SEARCHED FOR CASE STUDY B

Hyperparameter	Search Space	Search Result
GRU hidden layer size	[16, 32, 64]	16
Number of GRU layers	[1, 2, 3, 4]	4
Number of MLP layers	[1, 2, 3, 4]	3
GRU dropout rate	0.0 - 0.8	0.0
MLP dropout rate	0.0 - 0.8	0.2
Learning rate	1e-4 - 1e-2	0.00819
Weight decay	1e-5 - 1e-2	0.00002

based on the number of customers who would lose power if the line were removed from the network. Each repair team spends a few hours at each broken line to simulate the repair process. The episode concludes when all broken lines have been repaired.

6) *Dataset Organization and Model Training*: The hazard simulated in this case study is thunderstorms, which often occur in the summer; therefore, the time embedding is omitted from the input. To extract a uniform weather representation for all the substation service areas as the input to the GRU model, the weather input dimension must be fixed. We clustered all the centers of the power lines using K-Means and used the centroid locations to resample the wind speed field. A vector in  $\mathbb{R}^{16}$  for each substation service area was extracted as the uniform weather representation. The system embedding is the one-hot encoding of the substation service area. Note that the start and end times of the events in this case correspond to the start and end times of the thunderstorms, rather than the outage events. The resilience of substation service area  $k$  under hazard  $i$ ,  $Rs_{i,k}$ , is calculated using the resilience trapezoid method and is used as the ground truth for training and testing. Only the data from substation service areas where wind gusts occurred were used for training and resilience calculation.

Among all the data, 80% were used for training and validation, and 20% for testing. During the data split, we used stratified splitting; for each substation service area, 60% of the data were used for training, 20% for validation, and 20% for testing. On average, each substation service area had 422 data samples. All models were trained for 200 epochs. The model with the lowest loss in each fold was selected for testing. Hyperparameters were searched, and the best hyperparameters were selected based on the validation loss, as shown in Table III. The best models using the optimal hyperparameters achieved an MAE loss of 0.009892 on the validation set and 0.009987 on the test set.

7) *Resilience Evaluation*: The benchmark dataset comprises all the hazardous weather scenarios for all the substation service areas in the test set. Each substation service area is tested against the benchmark dataset using the trained models. The average of the test results for each substation service area is taken as the predicted resilience. The resilience estimates from the simulation and the trained GRU models are compared in Fig. 10. Note that the weather scenarios used to produce these two sets of results differ. The weather scenarios used to produce the simulation results are unique to each substation service area (about 422 scenarios for each). In contrast, the

resilience estimated using the proposed method utilized the benchmark dataset to test all the substation service areas (about 4643 weather scenarios). As shown in the figure, the predicted resilience follows the same trend as the simulation results (Spearman rank correlation coefficient is 0.839, with a p-value of  $1.234 \times 10^{-15}$ ). These results demonstrate the efficacy of the proposed method.

## V. CONCLUSION

In this work, we proposed a deep learning-based method for evaluating the resilience of power systems, which combines the advantages of statistics-based and simulation-based approaches. A deep learning model was designed and trained to estimate system performance based on severe weather scenarios and system information. The system's resilience was calculated as the average of the system's performance tested against a benchmark dataset containing multiple severe weather scenarios. Socio-economic and demographic factors were incorporated to produce a weighted resilience metric that reflects the consideration of socially vulnerable groups impacted by long-duration power outages. Two case studies were conducted to demonstrate the effectiveness of the proposed method and the utility of the resilience evaluation results in resilience enhancement planning.

## REFERENCES

- [1] "Weather-related power outages rising," <https://www.climatecentral.org/climate-matters/weather-related-power-outages-rising>, accessed: 2024-05-28.
- [2] D. K. Mishra, M. J. Ghadi, A. Azizivahed, L. Li, and J. Zhang, "A review on resilience studies in active distribution systems," *Renewable and Sustainable Energy Reviews*, vol. 135, p. 110201, 2021.
- [3] W. Li, *Risk assessment of power systems: models, methods, and applications*. John Wiley & Sons, 2014.
- [4] A. Azizivahed, S. Ghavidel, M. J. Ghadi, L. Li, and J. Zhang, "A novel reliability oriented bi-objective unit commitment problem," in *2017 Australasian Universities Power Engineering Conference (AUPEC)*. IEEE, 2017, pp. 1–6.
- [5] X. Liu, M. Shahidehpour, Z. Li, X. Liu, Y. Cao, and Z. Bie, "Microgrids for enhancing the power grid resilience in extreme conditions," *IEEE Transactions on Smart Grid*, vol. 8, no. 2, pp. 589–597, 2016.
- [6] Z. Bie, Y. Lin, G. Li, and F. Li, "Battling the extreme: A study on the power system resilience," *Proceedings of the IEEE*, vol. 105, no. 7, pp. 1253–1266, 2017.
- [7] E. Hossain, S. Roy, N. Mohammad, N. Nawar, and D. R. Dipta, "Metrics and enhancement strategies for grid resilience and reliability during natural disasters," *Applied energy*, vol. 290, p. 116709, 2021.
- [8] M. B. Ulak, A. Yazici, and E. E. Ozguven, "A prescriptive model to assess the socio-demographics impacts of resilience improvements on power networks," *International journal of disaster risk reduction*, vol. 51, p. 101777, 2020.
- [9] Z. Yu, M. Wang, Y. Yang, S. Wu, Q. Lu, Y. Zhu, Y. Liu, W. Wang, and C. Fang, "A data-driven framework of resilience evaluation for power systems under typhoon disasters," in *2022 IEEE International Conference on Industrial Engineering and Engineering Management (IEEM)*, 2022, pp. 1043–1047.
- [10] M. Panteli, P. Mancarella, D. N. Trakas, E. Kyriakides, and N. D. Hatzigiorgiou, "Metrics and quantification of operational and infrastructure resilience in power systems," *IEEE Transactions on Power Systems*, vol. 32, no. 6, pp. 4732–4742, 2017.
- [11] J. Dugan and S. Mohagheghi, "Assessment of social vulnerability to long-duration power outages in the united states," in *2023 IEEE Green Technologies Conference (GreenTech)*. IEEE, 2023, pp. 123–127.
- [12] J. Dugan, D. Byles, and S. Mohagheghi, "Social vulnerability to long-duration power outages," *International Journal of Disaster Risk Reduction*, vol. 85, p. 103501, 2023.



- [13] M. B. Ulak, A. Yazici, E. E. Ozguven, A. Vanli, and R. Arghandeh, "Power resilience assessment from physical and socio-demographic perspectives," in *2019 4th International Conference on System Reliability and Safety (ICSRS)*. IEEE, 2019, pp. 421–428.
- [14] F. Gerges, R. H. Assaad, H. Nassif, E. Bou-Zeid, and M. C. Boufadel, "A perspective on quantifying resilience: Combining community and infrastructure capitals," *Science of the Total Environment*, vol. 859, p. 160187, 2023.
- [15] C. Mazur, Y. Hoegerle, M. Brucoli, K. van Dam, M. Guo, C. N. Markides, and N. Shah, "A holistic resilience framework development for rural power systems in emerging economies," *Applied Energy*, vol. 235, pp. 219–232, 2019.
- [16] C. Brelsford, S. Tennille, A. Myers, S. Chinthavali, V. Tansakul, M. Denman, M. Coletti, J. Grant, S. Lee, K. Allen *et al.*, "A dataset of recorded electricity outages by united states county 2014–2022," *Scientific Data*, vol. 11, no. 1, p. 271, 2024.
- [17] M. Abdelmalak, S. Ericson, J. Cox, M. Ben-Idris, and E. Hotchkiss, "A power outage data informed resilience assessment framework," in *2022 Resilience Week (RWS)*. IEEE, 2022, pp. 1–6.
- [18] M. Abdelmalak, J. Cox, S. Ericson, E. Hotchkiss, and M. Benidris, "Quantitative resilience-based assessment framework using eagle-i power outage data," *IEEE Access*, vol. 11, pp. 7682–7697, 2023.
- [19] S. M. Lee, S. Chinthavali, N. Bhusal, N. Stenvig, A. Tabassum, and T. Kuruganti, "Quantifying the power system resilience of the us power grid through weather and power outage data mapping," *IEEE Access*, 2023.
- [20] L. Shen, B. Cassottana, and L. C. Tang, "Statistical trend tests for resilience of power systems," *Reliability Engineering & System Safety*, vol. 177, pp. 138–147, 2018.
- [21] L. Shen, Y. Tang, and L. C. Tang, "Understanding key factors affecting power systems resilience," *Reliability Engineering & System Safety*, vol. 212, p. 107621, 2021.
- [22] M. Amirioun, F. Aminifar, H. Lesani, and M. Shahidehpour, "Metrics and quantitative framework for assessing microgrid resilience against windstorms," *International Journal of Electrical Power & Energy Systems*, vol. 104, pp. 716–723, 2019.
- [23] M. Panteli and P. Mancarella, "Modeling and evaluating the resilience of critical electrical power infrastructure to extreme weather events," *IEEE Systems Journal*, vol. 11, no. 3, pp. 1733–1742, 2015.
- [24] G. Hou, K. K. Muraleetharan, V. Panchaloganjan, P. Moses, A. Javid, H. Al-Dakheeli, R. Bulut, R. Campos, P. S. Harvey, G. Miller *et al.*, "Resilience assessment and enhancement evaluation of power distribution systems subjected to ice storms," *Reliability Engineering & System Safety*, vol. 230, p. 108964, 2023.
- [25] M. Cresta, F. M. Gatta, A. Geri, M. Maccioni, and M. Paulucci, "Resilience assessment in distribution grids: A complete simulation model," *Energies*, vol. 14, no. 14, p. 4303, 2021.
- [26] M. Abdelmalak, J. Thapa, and M. Benidris, "Resilience of power systems to ice storms: Analysis and quantification," in *2023 IEEE Power & Energy Society General Meeting (PESGM)*. IEEE, 2023, pp. 1–5.
- [27] D. K. Mishra, M. J. Ghadi, L. Li, J. Zhang, and M. Hossain, "Active distribution system resilience quantification and enhancement through multi-microgrid and mobile energy storage," *Applied Energy*, vol. 311, p. 118665, 2022.
- [28] J. Beyza and J. M. Yusta, "Characterising the security of power system topologies through a combined assessment of reliability, robustness, and resilience," *Energy Strategy Reviews*, vol. 43, p. 100944, 2022.
- [29] C. Shang, T. Lin, C. Li, K. Wang, and Q. Ai, "Joining resilience and reliability evaluation against both weather and ageing causes," *Renewable and Sustainable Energy Reviews*, vol. 152, p. 111665, 2021.
- [30] A. Senkel, C. Bode, and G. Schmitz, "Quantification of the resilience of integrated energy systems using dynamic simulation," *Reliability Engineering & System Safety*, vol. 209, p. 107447, 2021.
- [31] Z. Wang, T. Ding, W. Jia, C. Huang, C. Mu, M. Qu, M. Shahidehpour, Y. Yang, F. Blaabjerg, L. Li *et al.*, "Multi-stage stochastic programming for resilient integrated electricity and natural gas distribution systems against typhoon natural disaster attacks," *Renewable and Sustainable Energy Reviews*, vol. 159, p. 111784, 2022.
- [32] H. Wang, K. Hou, J. Zhao, X. Yu, H. Jia, and Y. Mu, "Planning-oriented resilience assessment and enhancement of integrated electricity-gas system considering multi-type natural disasters," *Applied Energy*, vol. 315, p. 118824, 2022.
- [33] M. Ouyang and Z. Wang, "Resilience assessment of interdependent infrastructure systems: With a focus on joint restoration modeling and analysis," *Reliability Engineering & System Safety*, vol. 141, pp. 74–82, 2015.
- [34] H. Hafeznia and B. Stojadinović, "Resq-ios: An iterative optimization-based simulation framework for quantifying the resilience of interdependent critical infrastructure systems to natural hazards," *Applied Energy*, vol. 349, p. 121558, 2023.
- [35] S. Balakrishnan and B. Cassottana, "Infrarisk: An open-source simulation platform for resilience analysis in interconnected power–water–transport networks," *Sustainable Cities and Society*, vol. 83, p. 103963, 2022.
- [36] J. Xie, I. Alvarez-Fernandez, and W. Sun, "A review of machine learning applications in power system resilience," in *2020 IEEE Power & Energy Society General Meeting (PESGM)*. IEEE, 2020, pp. 1–5.
- [37] F. Yang, M. Koukoulas, S. Emmanouil, D. Cerrai, and E. N. Anagnostou, "Assessing the power grid vulnerability to extreme weather events based on long-term atmospheric reanalysis," *Stochastic Environmental Research and Risk Assessment*, vol. 37, no. 11, pp. 4291–4306, 2023.
- [38] S. Madasthu, A. Al Mamun, A. Abbas, E. Abbate, B. Chowdhury, and R. Cox, "Ensemble deep learning model for power system outage prediction for resilience enhancement," in *2023 North American Power Symposium (NAPS)*. IEEE, 2023, pp. 1–6.
- [39] K. Li, J. Ma, J. Gao, C. Xu, W. Li, Y. Mao, and S. Jiang, "Resilience assessment of urban distribution network under heavy rain: A knowledge-informed data-driven approach," *IEEE Access*, 2023.
- [40] S. Lee, J. Choi, G. Jung, A. Tabassum, N. Stenvig, and S. Chinthavali, "Predicting power outage during extreme weather events with eagle-i and nws datasets," in *2023 IEEE 24th International Conference on Information Reuse and Integration for Data Science (IRI)*. IEEE, 2023, pp. 211–212.
- [41] P. Gautam, A. Sreejith, and B. Natarajan, "A transductive graph neural network learning for grid resilience analysis," in *2023 IEEE International Conference on Communications, Control, and Computing Technologies for Smart Grids (SmartGridComm)*. IEEE, 2023, pp. 1–6.
- [42] "Hhs empower map," <https://empowerprogram.hhs.gov/empowermap>, accessed: 2024-01-27.
- [43] E. P. James and S. G. Benjamin, "Observation system experiments with the hourly updating rapid refresh model using gsi hybrid ensemble-variational data assimilation," *Monthly Weather Review*, vol. 145, no. 8, pp. 2897–2918, 2017.
- [44] D. C. Dowell, C. R. Alexander, E. P. James, S. S. Weygandt, S. G. Benjamin, G. S. Manikin, B. T. Blake, J. M. Brown, J. B. Olson, M. Hu *et al.*, "The high-resolution rapid refresh (hrrr): An hourly updating convection-allowing forecast model. part i: Motivation and system description," *Weather and Forecasting*, vol. 37, no. 8, pp. 1371–1395, 2022.
- [45] E. P. James, C. R. Alexander, D. C. Dowell, S. S. Weygandt, S. G. Benjamin, G. S. Manikin, J. M. Brown, J. B. Olson, M. Hu, T. G. Smirnova *et al.*, "The high-resolution rapid refresh (hrrr): An hourly updating convection-allowing forecast model. part ii: Forecast performance," *Weather and Forecasting*, vol. 37, no. 8, pp. 1397–1417, 2022.
- [46] B. K. Blaylock, "Herbie: Retrieve Numerical Weather Prediction Model Data," May 2024. [Online]. Available: <https://doi.org/10.5281/zenodo.11111866>
- [47] K. Cho, B. Van Merriënboer, C. Gulcehre, D. Bahdanau, F. Bougares, H. Schwenk, and Y. Bengio, "Learning phrase representations using rnn encoder-decoder for statistical machine translation," *arXiv preprint arXiv:1406.1078*, 2014.
- [48] D. P. Kingma and J. Ba, "Adam: A method for stochastic optimization," *arXiv preprint arXiv:1412.6980*, 2014.
- [49] R. Liaw, E. Liang, R. Nishihara, P. Moritz, J. E. Gonzalez, and I. Stoica, "Tune: A research platform for distributed model selection and training," *arXiv preprint arXiv:1807.05118*, 2018.
- [50] T. Akiba, S. Sano, T. Yanase, T. Ohta, and M. Koyama, "Optuna: A next-generation hyperparameter optimization framework," in *Proceedings of the 25th ACM SIGKDD International Conference on Knowledge Discovery and Data Mining*, 2019.
- [51] "How many watts does it take to run a house?" <https://www.energysage.com/electricity/house-watts/>, accessed: 2024-04-30.
- [52] C. Zhai, T. Y.-j. Chen, A. G. White, and S. D. Guikema, "Power outage prediction for natural hazards using synthetic power distribution systems," *Reliability Engineering & System Safety*, vol. 208, p. 107348, 2021.
- [53] OpenStreetMap contributors, "Planet dump retrieved from <https://planet.osm.org>," 2023, accessed on Oct. 24, 2023. [Online]. Available: <https://www.openstreetmap.org>